TENSILE BEHAVIOUR OF DUCTILE STEEL FIBRE/EPOXY COMPOSITES

M. G. Callens[1], L. Gorbatikh[1] and I.Verpoest[1]

[1]*Department of Metallurgy and Materials Engineering, KULeuven, Kasteelpark Arenberg 44, B-3001 LEUVEN (Belgium)*

Keywords: Steel fibre, polymer composite, failure behaviour, tensile tests

Abstract
A common limitation of structural fibre-reinforced polymers is their low toughness and ductility. This is due to the intrinsic brittleness of conventional fibres. In the present work we use a new type of fibres – annealed stainless steel fibres that combine a high stiffness and a high strain-to-failure. The study investigates the tensile behaviour of unidirectional (UD) and cross-ply composites produced from steel fibres and epoxy resin. It was found that the steel fibre epoxy composites exhibit a strain-to-failure 4 times higher than a typical carbon composite and almost 3 times higher than a typical glass fibre composite. To understand the failure behaviour of ductile fibre/epoxy composites we also used simple micromechanical models based on the constituent materials.

1 Introduction
The strain-to-failure of structural fibre-reinforced polymers like carbon or glass fibre composites is known to be low. The reason for this is brittleness of the fibres. The composite ductility (and overall toughness) can be enhanced by choosing fibres that have a higher strain-to-failure. It has already been proven in such systems as metal fibre reinforced ceramics, metal fibre reinforced metals and short ductile fibre reinforced polymers [1-3]. In fiber-reinforced composites the choice of ductile fibres is limited to polymeric fibres (i.e. aramid, polyethylene fibers) or natural fibres (i.e. silk, coconut fibers [4,5]). High toughness of these fibres, however, comes at the cost of low stiffness, which limits their use in structural applications.

Recently a new class of stiff but ductile fibres became available for application in composites: steel fibres (diameter 5 - 100 µm) which exhibit both high stiffness (approx. 193 GPa) and high strain-to-failure (up to 20%). The stiffness of these new fibres is almost as high as that of a carbon fibre, but combined with a strain-to-failure as high as that of a silk fibre.

The current study focuses on the tensile behaviour of ductile continuous stainless steel fibres, with a diameter of 30 µm, embedded in an epoxy matrix. The tensile behaviour is investigated for uni-directional (UD) and cross-ply laminates. The failure behaviour of these composites is of particular interest.

Conventional fibres like carbon and glass fibres have an almost perfect linear behaviour until failure. Any large non-linearity in a stress-strain diagram of these composites can only be attributed to the non-linear behaviour of the matrix or accumulated damage. This is not the

case for the ductile steel fibres which undergo plastic deformation at small strains. The damage development is investigated by means of the acoustic emission technique [6-9].

This research also employs simple modelling to separate the non-linear behaviour of the ductile steel fibres and the matrix from the damage occurring in a composite laminate under static tensile loading. The modelling is used as a tool to understand how the composite behaviour is affected by exchanging the brittle fibres by ductile fibres. This is a first step in the understanding of the failure behaviour of ductile steel fibre/epoxy composites.

2 Materials and methods

2.1 Raw materials

The reinforcement is a quasi UD woven structure consisting of steel fibre warp yarns (each containing 550 fibres) and a thin polyethylene terephthalate (PET) weft yarn (Figure 1). The reinforcement is supplied by N.V. Bekaert S.A.. The annealed steel fibres have a diameter of 30 µm and are made of a 316 stainless steel alloy.

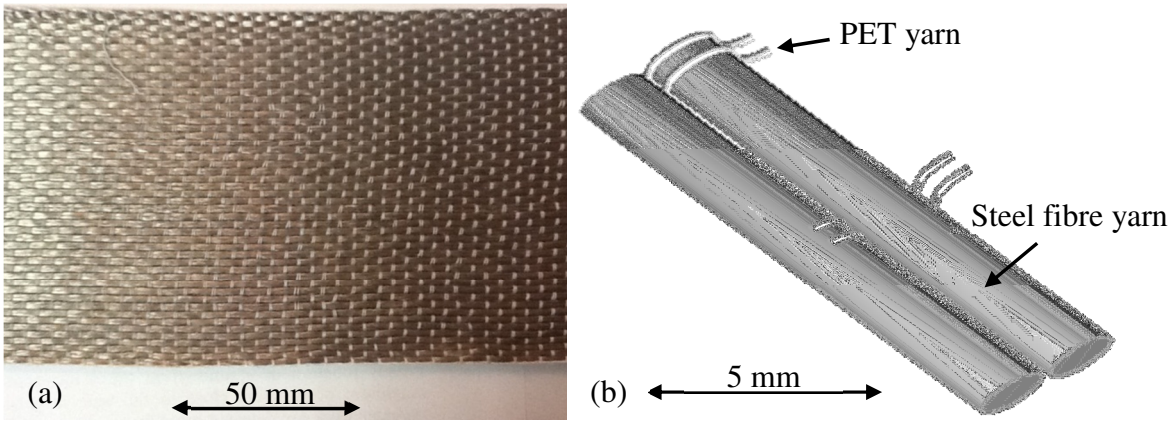

Figure 1. (a) Photograph of the quasi UD woven structure. (b) Unit cell of the quasi UD woven structure, bundle of 550 steel fibres in grey, PET weft yarn in white.

The stress-strain curve of individual fibres was tested at NV Bekaert SA (Figure 2). The mechanical properties of a single fibre are reported in table 1. Epikote 828LVEL (a Bisphenol-A type) is used as epoxy resin, with a 1,2-diaminocyclohexane (Dytek DCH-99) as hardener (15,2 / 100). The tensile properties of the epoxy resin (Figure 2) were tested at Vrije Universiteit Brussel.

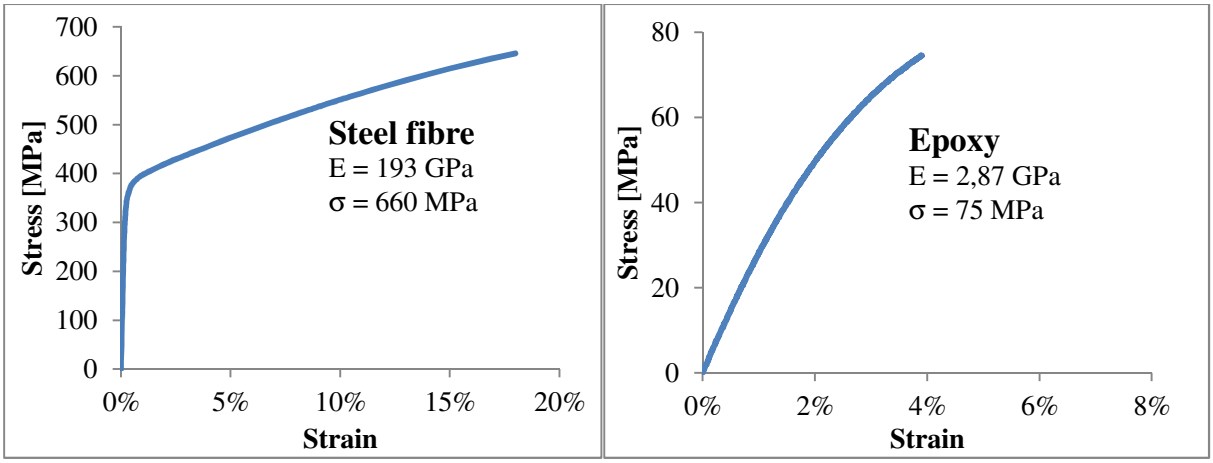

Figure 2. Typical stress-strain curve of a single stainless steel fibre.

2.2 Production of the composite plates

Three layers of the of quasi UD structure are stacked for the UD laminate. The stacking configuration of the cross-ply laminate is $(0,90)_s$.The composite plates are produced using vacuum assisted resin infusion. The impregnation is done at 40°C and the epoxy is cured for 1h at 70°C and post-cured for 1h at 150°C. The fibre volume fraction of the UD laminate is 43,96 ± 0,97 % and of the cross-ply laminate, 42,04 ± 1,50 %. It is calculated based on the areal weight of the fabric and the thickness of the composite.

2.3 Experimental methodology

The UD and cross-ply composite plates are tested under quasi static tensile loading. The tests are performed according to ASTM D3039 on an Instron 4505. The displacement is controlled (2 mm/min) and the loading is measured using a 100 kN load cell.

The strain is measured using an optical extensometer. This technique uses a camera that takes digital images of the central region of the sample every 500 µs during the test. Digital image correlation software Vic2D (LIMESS Messtechnik und Software GmbH) is used to calculate the average strain on the surface of the sample.

During the tensile loading of the cross-ply laminate the damage progression is evaluated using acoustic emission registration. Two acoustic sensors (V5375-M) at the surface of the sample are used to detect sound waves, one at each end of the tensile sample. The energy of the AE events is recorded by VALLEN system and plotted as a function of strain.

2.4 Modelling methodology

Simple micromechanical modelling is used to understand the elasto-plastic behaviour of steel fiber composites. Three approximations are proposed. In the first approximation we assume that only the longitudinal fibres carry the load. The stress-strain curve of the fibre can thus be scaled with the fibre volume fraction according to the linear rule of mixture (isostrain assumption):

$$\sigma_{composite} = V_f \cdot \sigma_{fibre} \ , \tag{1}$$

where $\sigma_{composite}$ represents the stress-strain curve in the composite, V_f the fibre volume fraction and σ_{fibre} the stress-strain curve of a single fibre.

In a second approximation, the stress-strain curve of the matrix is added, also according to the linear rule of mixture (isostrain assumption):

$$\sigma_{UD\ composite} = V_f \cdot \sigma_{fibre} + \left(1 - V_f\right) \cdot \sigma_{epoxy} \ , \tag{2}$$

where $\sigma_{UD\ composite}$ represents the stress-strain curve in the UD composite and σ_{epoxy} the stress-strain curve of the epoxy matrix.

For the cross-ply laminate, the transverse ply is accounted for by adding an experimental tensile curve of a UD composite in the transverse direction:

$$\sigma_{cross-ply\ composite} = \frac{1}{2}\left(V_f \cdot \sigma_{fibre} + \left(1 - V_f\right) \cdot \sigma_{epoxy}\right) + \frac{1}{2}\sigma_{transverse\ ply} \ , \tag{3}$$

where $\sigma_{cross-ply\ composite}$ represents the stress-strain curve in the cross-ply composite and $\sigma_{transverse\ ply}$ the stress-strain curve of a 90° tensile test on a UD composite.

Formulas (2) and (3) can also be used to determine the in situ behaviour of the matrix (in the UD composite) and the 90° ply (in the cross-ply composite), respectively. This is done by fitting the modelled stress-strain curve to the experimentally measured one. This modelling approach can help us understand when the onset of damage begins and how it affects the tensile behaviour. These approximations assume that the longitudinal fibres remain undamaged.

The in situ behaviour of the 90° ply can be compared to the AE data. This is to check whether the strain at which damage is assumed to start deteriorating the tensile behaviour is also the strain at which first AE events occur.

3 Results and discussion

3.1 UD composite

3.1.1 Mechanical properties

Table 1 reports the tensile properties of the UD steel fibre composite. In the fiber direction it exhibits a strain-to-failure 4 times higher than a typical UD carbon composite and almost 3 times higher than a typical UD glass fibre composite The full potential of the strain-to-failure of the steel fibres (±17 %) is, however, not yet realized in this UD composite.

3.1.2 Modelling results

Figure 3 (a) shows the experimental and modelled stress-strain curves. There is a large discrepancy between the measured stress-strain curve and the downscaled stress-strain curve of a steel fibre, which is the first approximation. The matrix seems to carry a significant portion of the load up to the composite final failure. Even at 7% strain, at the failure of the UD composite, the first approximation predicts a 20 MPa lower stress. The latter can be attributed to the matrix contribution.

The second approximation, which includes the experimental stress-strain curve for the epoxy matrix, follows the experimental curve closely until about 2,5% strain. From 2,5% strain on, the contribution of the matrix is overestimated. The stress is overestimated because damage in the form of matrix cracks or local fiber debonds are not included in the model. From this exercise we conclude that damage is likely to occur only after the onset of plastic deformation of the steel fibres (at about 0,4% strain).

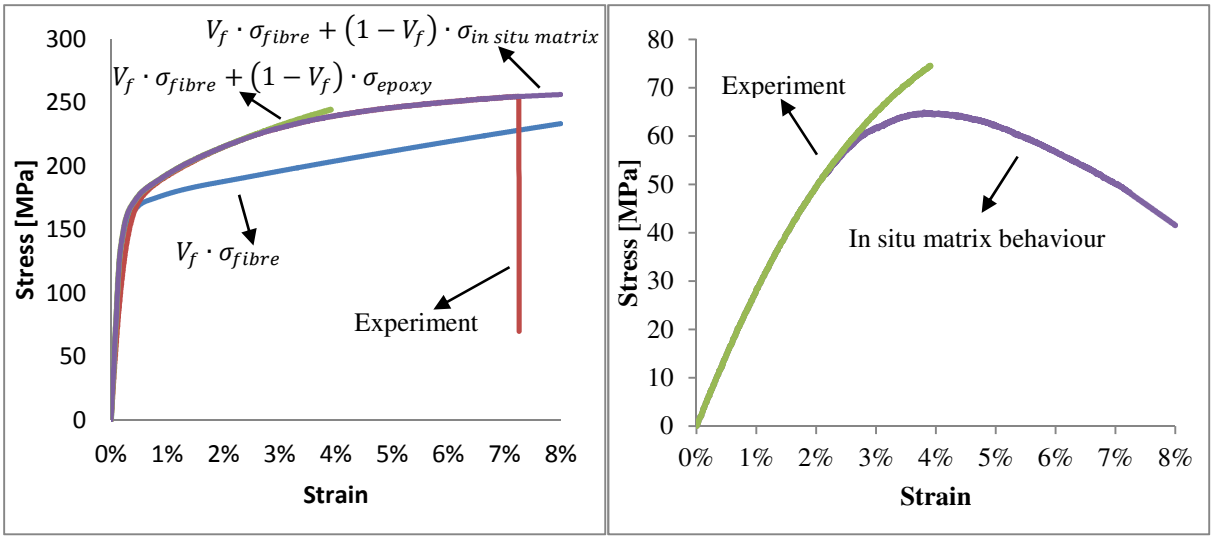

Figure 3. (a) Typical stress-strain curve of the UD steel fibre composite tested in the longitudinal direction and modelling curves to understand the elasto-plastic tensile behaviour. (b) Stress-strain curve of the Epikote 828 LVEL resin and in situ behaviour of the matrix.

Figure 3 (b) shows two tensile curves for the epoxy matrix. The first curve is the experimentally measured tensile curve of the epoxy, which is used in the second approximation of the UD tensile curve. The second curve represents the in situ matrix behaviour in order to fit the model curve to the UD tensile curve.

The in situ matrix behaviour follows the experimental epoxy curve quite accurate until 2,5% strain. Despite the fact that damage could already be present from about 2,5 %, the epoxy still carries a significant amount of load until final failure (at 7%) of the UD composite even though the measured strain-to-failure of the pure epoxy is only 4%. This is possible because growth of cracks in the matrix is hindered by the steel fibres. As a result cracks are homogenously distributed in the composite. This is visible on the surface of a tested specimen because the cracks remain opened (± 50µm) due to the plastic deformed steel fibres.

To make full use of the potential of steel fibres, a more ductile matrix is needed. Further research is currently planned to investigate the effect of matrix ductility on the composite tensile behaviour.

3.2 Cross-ply composite

3.2.1 Mechanical properties

Table 1 reports the tensile properties of the cross-ply steel fibre composite. The strain-to-failure of the cross-ply composite is similar as the strain-to-failure of the UD composite while the strength of the cross-ply composite is slightly higher than half the strength of the UD composite.

3.2.2 Modelling results

Similarly to the UD composite case, figure 4 (a) shows the experimental stress-strain curve and the modelled curves. The first approximation, in which only the longitudinal fibres carry the load, again shows a significantly lower stress. Therefore, the second approximation assumes that the entire longitudinal plies carry the load. Also this second approximation shows a large deviation in stress compared to the experimental result.

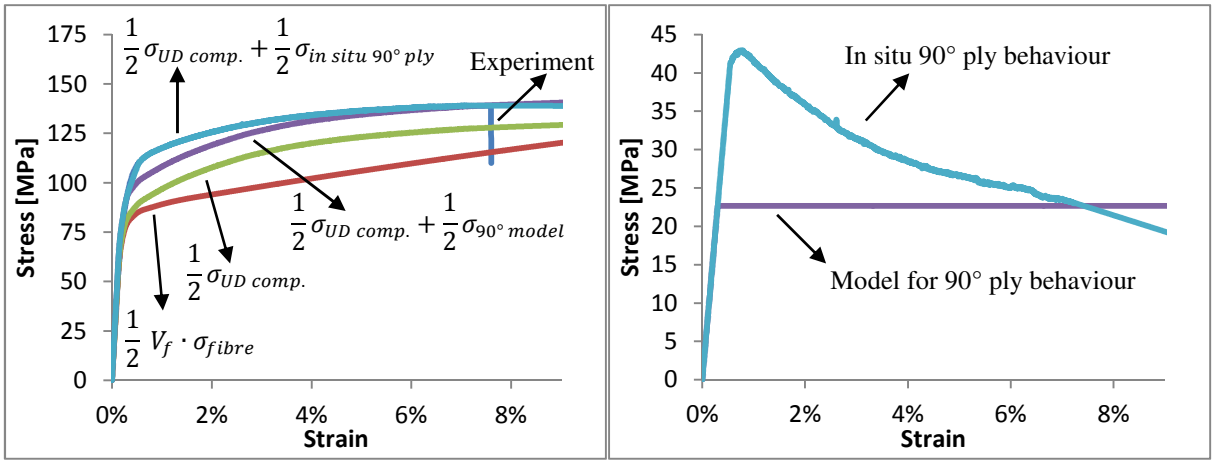

Figure 4. (a) Typical stress-strain curve of the cross-ply steel fibre composite and modelling curves to understand the elasto-plastic tensile behaviour. (b) Stress-strain curve of the model curves for the 90° ply within the cross-ply composite.

To account for the load contributed by the 90° plies a simple 90° stress-strain curve is created. The model is based on actual 90° ply measurements (Table 1) and consists of a linear part up to 22 MPa, which is the average strength of a separate 90° ply. To account for damage in a transverse ply, the stress is kept constant at 22 MPa (Figure 4,b). The model results in a stress-strain curve of a cross-ply laminate that approaches the stress-strain curve of the experiment. However, from 0,5% till 4% strain there is still a significant discrepancy between the model and the experiment.

This means that the 90° plies contribute more than is assumed in the model for the 90° ply. The contribution of the 90° ply can be calculated using the difference between the UD stress-strain curve and the experimental cross-ply curve. This is shown by the in situ 90° ply behaviour (Figure 4 (b)) - behaviour of the 90° ply inside the cross-ply laminate.

The in situ 90° ply curve has a linear region up to about 45 MPa after which the stress slowly decreases. From this we can assume that the 90° ply remains unharmed up to 45 MPa. After this peak, damage develops in the 90° plies and the stress there drops. This is logical because the strength of a separate 90° ply is greatly influenced by local defects, while a 90° ply inside the cross-ply laminate is protected by the 0° plies surrounding it. Also a crack or local debonding will only locally lower the stress contributed by the 90° ply. While the number of cracks increases the total stress contributed by the 90° ply will slowly decrease.

The hypothesis, that the 90° ply remains unharmed until 45 MPa, can be checked using the acoustic emission data. Figure 5 shows the acoustic emission events and the cumulative acoustic emission energy together with the experimental stress-strain curve of the cross-ply composite and the in situ 90° ply behaviour. The first acoustic emission is still within the linear part of the in situ 90° ply behaviour, but the first jump to a higher energy level and an increase in acoustic events occurs at the same strain level as the peak in the in situ 90° ply behaviour. This first transition to higher energies is often referred to as damage initiation threshold and can be attributed to the onset of transverse cracks [6]. The stress in the 90° ply decreases after the damage initiation threshold and the cumulative acoustic energy increases.

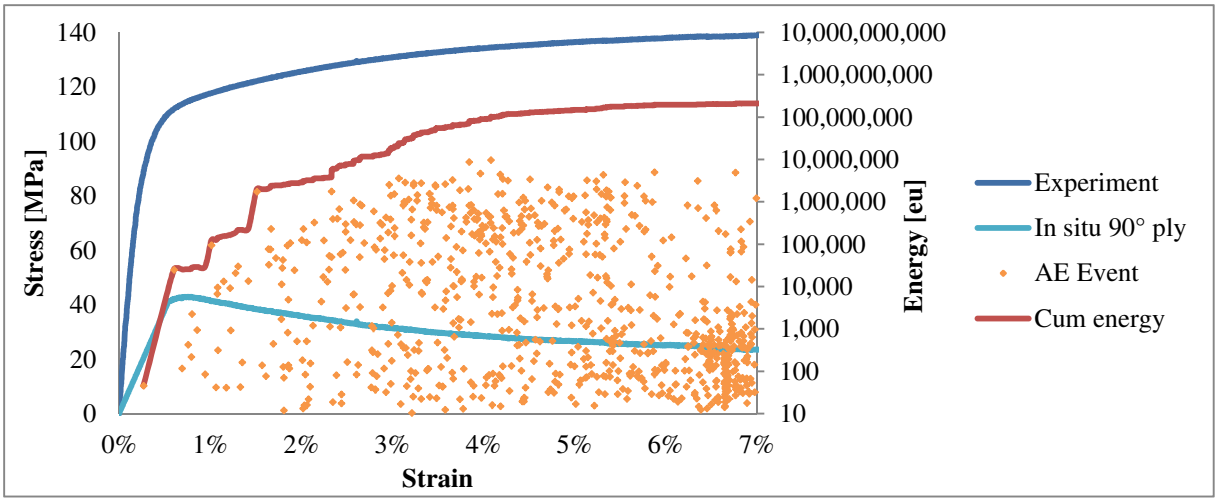

Figure 5. Stress-strain curve of the experimental cross-ply composite, single acoustic emission events, cumulative acoustic emission curve and expected 90° ply behaviour.

It is expected that the strain-to-failure of the cross-ply composite will improve with a more ductile matrix. A more ductile matrix should allow the steel fibres to deform further, enhancing the strain-to-failure of the composite. A strong fibre/matrix interphase to limit the debonding and transverse cracking in the 90° plies is also preferred.

	Vf	Nr. of specimens	E (GPa)	σ (MPa)	ε_{ult} (%)
UD 0°	43,96 ± 0,97 %	5	67,03 ± 2,42	259,63 ± 7,73	7,29 ± 0,31
UD 90°		5	7,59 ± 0,36	22,68 ± 1,52	0,30 ± 0,02
Cross-ply	42,04 ± 1,50 %	5	36,37 ± 5,54	138,21 ± 4,63	6,78 ± 1,01

Table 1. Mechanical properties of the UD and cross-ply steel fibre composites

4 Conclusion

It can be concluded that ductile steel fibres deliver composites with a high strain-to-failure (± 7%) both in case of UD and cross-ply composites. The steel fibre epoxy composite exhibits a strain-to-failure 4 times higher than a typical UD carbon composite and almost 3 times higher than a typical UD glass fibre composite. The full potential of the strain-to-failure of the steel fibres (±17 %) is, however, not yet realized in the composite. Further research is needed to find the most suitable matrix and fibre/matrix interphase.

Simple micromechanical models based on the constituent materials can reproduce the stress-strain diagram of both the UD and cross-ply composites until the onset of damage. This has been verified using acoustic emission in case of the cross-ply steel fibre composites.

5 Acknowledgements

The work at K.U.Leuven was performed in the scope of the SIM Nanoforce (Next generation nano-engineered polymer-Steel/carbon nanotube hybrids) program through the NaPoS project. The authors would like to thank S. Vandewalle and P Persoone from NV Bekaert SA for supplying the steel fibre reinforcement and A.K. Ghosh and B Van Mele from the Vrije Universiteit Brussel for characterizing the mechanical properties of the epoxy. The help of technicians K. Van de Staey, B. Pelgrim and M. Adams is gratefully acknowledged.

6 References

[1] Hoffman M, Fiedler B, Emmel T, Prielipp H,Claussen N,Gross D, Rodel J, Fracture behaviour in metal fibre reinforced ceramics, Acta Materialia, 1997, 45(9): 3609-3623

[2] Tardiff G Jr., Fracture mechanics of brittle matrix ductile fiber composites, Engineering Fracture Mechanics, 1973, 5(1): 1-10

[3] Wetherhold RC and Bos J, Ductile reinforcements for enhancing fracture resistance in composite materials, Theoretical and Applied Fracture Mechanics, 2000, 33(2): 83-91

[4] J. Vanderbeke, A.W. Van Vuure and I. Verpoest, Designing natural silk fibre reinforced thermoplastic composites as tough composite materials against low velocity impact, Proc. European SAMPE symposium, March 2008, Paris, 6p.

[5] A.W. Van Vuure, J. Vanderbeke, L. Osorio, E. Trujillo, C. Fuentes and I. Verpoest, Natural Fibre Composites: Tough (silk) and strong (bamboo), Proc. ICCM-17, Edinburgh, July 2009, 8 p.

[6] Lomov SV, Ivanov DS, Truong TC, Verpoest I, Baudry F, Vanden Bosche K, Xie H, Experimental methodology of study of damage initiation and development in textile composites in uniaxial tensile test. Comp Sci Tech, 2008, 68: 2340-2349

[7] Ivanov DS, Lomov SV, Bogdanovich AE, Mungalov D, Karahan M, Verpoest I, A comparative study of tensile properties of non-crimp 3D orthogonal weave and multi-layer plain weave E-glass composites. Part 1: Materials, methods and principal results. Composites Part A, 2009, 40(8): 1134–1143

[8] Lomov SV, Bogdanovich AE, Ivanov DS, Mungalov D, Karahan M, Verpoest I, A comparative study of tensile properties of non-crimp 3D orthogonal weave and multi-layer plain weave E-glass composites. Part 1: Materials, methods and principal results. Composites Part A, 2009, 40: 1134–1143

[9] Ivanov DS, Lomov SV, Bogdanovich AE, Karahan M, Verpoest I, A comparative study of tensile properties of non-crimp 3D orthogonal weave and multi-layer plain weave E-glass composites. Part 2: Comprehensive experimental results. Composites Part A, 2009, 40: 1144–1157